MATERIALS SCIENCE

Nanomesh pressure sensor for monitoring finger manipulation without sensory interference

Sunghoon Lee[1], Sae Franklin[2], Faezeh Arab Hassani[1]*, Tomoyuki Yokota[1], Md Osman Goni Nayeem[1], Yan Wang[1], Raz Leib[3], Gordon Cheng[2], David W. Franklin[3], Takao Someya[1,4]†

Monitoring of finger manipulation without disturbing the inherent functionalities is critical to understand the sense of natural touch. However, worn or attached sensors affect the natural feeling of the skin. We developed nanomesh pressure sensors that can monitor finger pressure without detectable effects on human sensation. The effect of the sensor on human sensation was quantitatively investigated, and the sensor-applied finger exhibits comparable grip forces with those of the bare finger, even though the attachment of a 2-micrometer-thick polymeric film results in a 14% increase in the grip force after adjusting for friction. Simultaneously, the sensor exhibits an extreme mechanical durability against cyclic shearing and friction greater than hundreds of kilopascals.

Precise measurement of finger manipulation is critical to understand and reproduce the sense of natural touch for applications in prosthetic hands (*1*, *2*), human-machine interaction (*3*, *4*), clinical restoration of hand function (*5*, *6*), and digital archiving of a craftsman's skills (*7*, *8*). Advances in examining the sense of touch have come from optical-based estimation of finger forces based on nail color (*9*, *10*), force sensor–integrated objects (*11*), and instrumented gloves (*12*–*16*). An application of soft and flexible sensors to the fingertip enabled direct measurement of the force between the finger and other objects (*17*–*19*); the mechanical properties of the sensors decreased physical interferences that would arise from the mechanical mismatch between the skin and sensors. Furthermore, use of elastomeric substrates (*20*, *21*) and/or a reduction in sensor thickness (*22*, *23*) has substantially improved the conformability of sensors to the skin and enabled more accurate monitoring of finger touch. Recently, ultrathin (a few micrometers) sensors have been demonstrated, which reduce the loss in sensation (*24*–*26*). However, the challenge is to monitor finger touch without losing any touch sensation (*27*). Covering the human finger with any object, even a superthin layer, causes substantial degradation of natural touch, affecting the sensory information and distorting the inherent control (*28*–*30*).

[1]Department of Electrical Engineering and Information Systems, School of Engineering, The University of Tokyo, 7-3-1 Hongo, Bunkyo-ku, Tokyo 113-8656, Japan. [2]Institute for Cognitive Systems, Department of Electrical and Computer Engineering, Technical University of Munich, Karlstraße 45/II, 80333 München, Germany. [3]Neuromuscular Diagnostics, Department of Sport and Health Sciences, Technical University of Munich, Georg-Brauchle-Ring 60/62, 80992 München, Germany. [4]Institute for Advanced Study, Technical University of Munich, Lichtenbergstrasse 2a, 85748 Garching, Germany.
*Present address: Department of Electrical and Electronic Engineering, University of Bristol, Bristol, UK.
†Corresponding author. Email: someya@ee.t.u-tokyo.ac.jp

We monitor force using sensors directly attached to the highly sensitive fingertip. To minimize sensory interference, we developed ultrathin nanomesh sensors composed of compliant nanoporous structures. Figure 1, A and B, shows an optical image of a pressure sensor on a fingertip and the cross-sectional scanning electron microscopic (SEM) image of the sensor formed on polyimide film, respectively. The nanomesh sensor consists of the following four layers: (i) a polyurethane nanomesh–embedded passivation layer, (ii) a top Au nanomesh electrode layer, (iii) a parylene-coated polyurethane nanomesh intermediate layer, and (iv) a bottom Au nanomesh electrode layer. The four layers are laminated in sequence onto objects, such as skin, without other substrates.

The bottom and top Au nanomesh layers are prepared by using electrospun polyvinyl alcohol (PVA) nanofibers as a sacrificial supporting layer (*31*). The intermediate and passivation layers are made of polyurethane nanofibers that have a diameter in the range of 200 to 400 nm. In the case of the intermediate layer, an additional 200-nm-thick parylene layer is deposited around polyurethane nanofibers. An air gap between the bottom Au electrode layer and the intermediate layer is formed, as shown in Fig. 1B. To ensure mechanical durability while keeping the sensor thin, a passivation layer of polyurethane nanofibers attached with dissolved PVA nanofibers is introduced. The thickness of the intermediate and the passivation layers are ~10.5 and 2.5 μm, respectively. The detailed structure is described in the materials and methods (see also fig. S1).

Layers can be bonded to each other after dissolution of the PVA nanofibers by water mist (fig. S2). When high pressure or shear force is applied, the layers do not detach from each other, maintaining the sensor structure and its functionalities (fig. S3). The top Au nanomesh layer shows a stable conductivity, even though it is formed on a porous and rough nanofiber surface (fig. S4). Therefore, the pressure applied to sensors can be monitored by the capacitance change between the bottom and top Au nanomesh electrodes, because of the deformation of the parylene-coated polyurethane nanomesh intermediate layer. In addition, the pressure sensitivity of the sensor is mainly determined by the mechanical properties of the intermediate layer. The parylene-coated polyurethane intermediate layer was selected for this sensor because it exhibits higher sensitivity compared with a sensor using the polyurethane-only intermediate layer (figs. S5 and S6).

Figure 2A shows the capacitance change of the sensor using the 200-nm parylene-coated polyurethane intermediate layer. The sensitivity (slope of the capacitance change–pressure curve) is 0.141 kPa^{-1} in the low-pressure range (<1 kPa) and 0.010 kPa^{-1} in the high-pressure range (>10 kPa). In addition to the nanomesh intermediate layer, the number of PVA nanofibers used to form the top Au nanomesh layer also affected the sensitivity of the sensor (figs. S7 and S8). When the number of PVA nanofibers was small (with an electrospinning time of 10 min), the sensitivity was 0.028 kPa^{-1}. By contrast, when the number of PVA nanofibers was large (with an electrospinning time of 50 min), the sensitivity decreased to 0.0014 kPa^{-1}. SEM observations showed that the porous structure of the intermediate layer was maintained after the smaller number of PVA nanofibers were dissolved on the surface of intermediate layer (fig. S8B). However, when the number of PVA nanofibers was large, the dissolved PVA filled the pores on the surface of the intermediate layer (fig. S8D). Therefore, to maintain the nanoporous structure of the intermediate layer, a small number of PVA nanofibers was used.

Nanomesh sensors maintained their functionality after repeated cyclic pressing. As shown in Fig. 2B and fig. S9, the change in the performance of the sensor was negligibly small, with a less than 0.15% decrease over 1000 cycles of pressing at 19.6 kPa (capacitance change of 0.658 on the first cycle and 0.659 on the 1000th cycle). In addition, the top Au nanomesh electrode maintained the conductivity without a considerable degradation during the repeated cyclic pressing.

To check the applied pressure dependence of the response time, three pressure levels (0.98, 4.9, and 19.6 kPa) were repeatedly applied for 2 s and released for 2 s while measuring the change in the sensor capacitance (fig. S10). As shown in Fig. 2, C and D, the sensor showed similar response times for each pressure, in which all showed a response time between 190 and 220 ms for the maximum capacitance change of 80%.

Furthermore, nanomesh sensors exhibited durability against friction. The functionality

of the sensors could be maintained even when the sensor surface was rubbed with a vertical pressure of more than 100 kPa. To evaluate the mechanical durability of the sensor against friction, experiments were carried out by repeatedly rubbing the surface of the sensor with a spherical polyurethane ball of 3-mm diameter (fig. S11). The friction force was controlled by an external load weight. When the surface of the sensor was rubbed 300 times with a 50-g weight, the change in electrical characteristics was negligibly small (relative capacitance of 0.997 after 300 cycles) (Fig. 3A). In addition, the nanomesh sensor still exhibited pressure sensitivity after the high friction was applied, for which the sensitivities were 0.077 kPa^{-1} (before friction) and 0.070 kPa^{-1} (after friction) with a change of less than 9.7% (Fig. 3B).

Figure 3, C to E, shows a dynamic change in capacitance during the cyclic friction application. During the rubbing of the nanomesh sensor surface with the polyurethane ball, pressure was applied to the sensor, resulting in an increase in the capacitance. In each cycle, the polyurethane ball passed through the sensor surface twice (forward and backward), resulting in two peaks for each cycle. Figure 3C shows all 300 cycles, and the peak amplitude was 6.63 pF for the first cycle and 6.34 pF for the 300th cycle. Although the amplitude was changed by 4.6%, the pressure due to the friction could be detected with minimal performance change of the pressure sensor properties (Fig. 3, D and E).

The durability of the nanomesh sensors was achieved by the introduction of the thin polyurethane nanomesh–embedded passivation layer. For comparison, a sensor comprising only three layers (top electrode layer, intermediate layer, and bottom Au electrode layer) without the polyurethane nanomesh–embedded passivation layer was prepared. Both sensors were rubbed 10 times by using different load weights between 10 and 100 g (fig. S12, A and B). The nanomesh sensor with the passivation layer showed a sufficiently small change in electrical properties regardless of the weight, such that the change in the sensor capacitance remained less than 4.1% compared with the initial sensor capacitance (fig. S12C). In the case of the sensor without the polyurethane nanomesh–embedded passivation layer, it showed a huge degradation in the sensor performance. The initial capacitance value (capacitance without pressing) was reduced by 79.7% when the surface was rubbed with a weight of 70 g or greater.

The functionality of the top Au nanomesh electrode was evaluated after the application of friction. The conductance of the nanomesh electrode, with and without the passivation layer, was measured after rubbing 10 times with the various friction loads (fig. S12D). For the sensor with the polyurethane nanomesh–

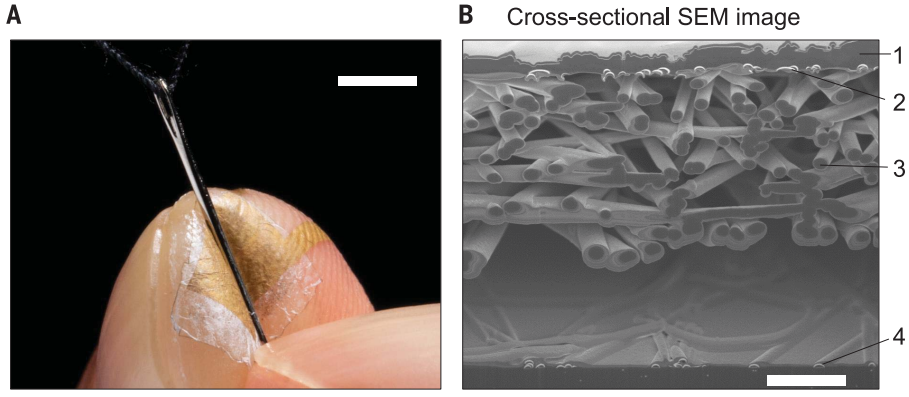

Fig. 1. Structure of the nanomesh pressure sensor. (**A**) Nanomesh pressure sensor attached to an index finger. Scale bar, 5 mm. (**B**) Cross-sectional SEM image of the nanomesh sensor laminated on polyimide film at a tilt angle of 52°. The sensor consists of four layers: a polyurethane nanomesh–embedded passivation layer (1), a top Au nanomesh electrode layer (2), a parylene-coated polyurethane nanomesh intermediate layer with an air gap (3), and a bottom Au nanomesh electrode layer (4). The surface of the sensor is covered by a protective layer during the SEM observation. Scale bar, 5 μm.

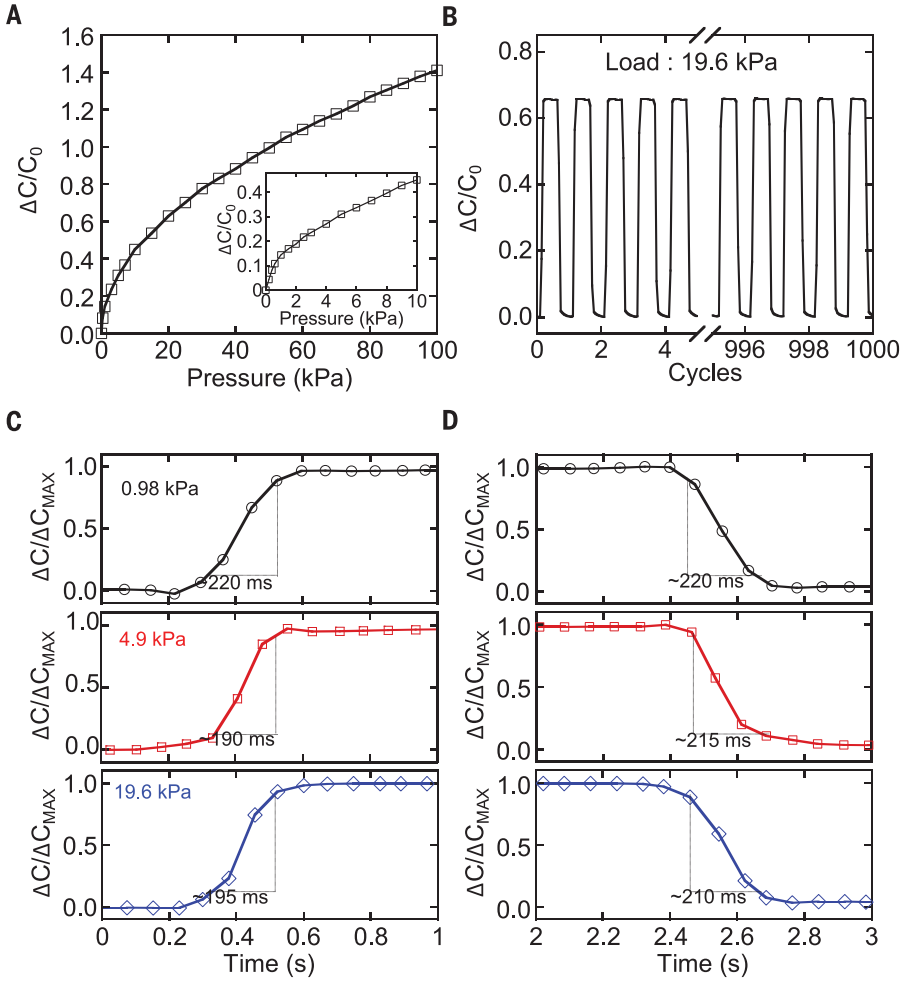

Fig. 2. Electrical characterization of nanomesh pressure sensor. (**A**) Relative capacitance change ($\Delta C/C_0$) as a function of pressure applied to sensor. The inset represents the pressure ranging from 0 to 10 kPa. (**B**) Pressure sensitivity of the nanomesh sensor during 1000 cyclic pressure applications. (**C** and **D**) Response time of the nanomesh sensor when pressing (C) and releasing (D) with three pressure levels (0.98, 4.9, and 19.6 kPa). The capacitance change is normalized by a maximum capacitance change (ΔC_{MAX}) at each pressure application.

embedded passivation layer, the conductance was slightly decreased from 0.0137 to 0.0119 S after the 100-g friction test. This conductance was sufficiently high to measure the capacitance of the sensor. However, in the case of the nanomesh electrode without the passivation layer, the conductance gradually decreased as the weight increased from 10 to 60 g and became less than 1.05×10^{-4} S after rubbing with the weight of 70 g. The SEM observations of the Au nanomesh surface showed that the Au nanomesh layer was partially delaminated when there was no passivation layer (fig. S13). The delaminated area increased with the increase in the friction weight, which was consistent with the change of conductivity.

To scientifically demonstrate the minimal effect of nanomesh sensors on human sensation, we conducted an object-grasping experiment. If the nanomesh material affects the sensory feedback from the finger, then participants will produce a larger grip force for the same load force (*27*, *30*). Eighteen participants grasped and lifted an instrumented object (four different masses) under seven different conditions: bare finger, three thicknesses of nanomesh material, and three thicknesses of parylene film (Fig. 4A). For each material condition and mass, participants produced 10 trials wherein they grasped the object with their thumb and index finger, lifted it, and held for 5 s. For objects with larger masses, the grip force increased (Fig. 4B). These grip forces were similar between the bare finger (red line) and all three nanomesh material thicknesses (blue lines) but were larger for the parylene film conditions (green lines). The same trend in the data can be seen for individual participants (Fig. 4, C and D). After a significant main effect of surface material ($F_{6,371}$ = 2.15, P = 0.04), mass ($F_{1,371}$ = 1425.37, P < 0.001), and their interaction ($F_{6,371}$ = 3.43, P = 0.0026) on the grip force values, post hoc tests were used to examine differences in the surface material. There were no significant differences between the bare finger and any of the nanomesh materials (all P = 1.0), whereas all three parylene film thicknesses exhibited larger grip forces than either the bare finger (all P < 0.001) or the nanomesh materials (all P < 0.001).

During object lifting, grip force increases both with decreasing sensory feedback and decreasing friction between the fingers and the object (*32*). The friction coefficient for each condition was measured by a slip ratio experiment (*27*) (see materials and methods). There was a main effect of surface material on the friction coefficient by using a general linear model ($F_{6,100}$ = 4.94, P < 0.001; Fig. 4E). To remove any potential friction effect, we subtracted the minimum grip force necessary based on the grasp friction coefficient and expressed the amount of grip force exceeding this level as a function of the material thickness (Fig. 4, F and G). There was a significant main effect of surface material ($F_{6,371}$ = 4.5, P < 0.001) and mass ($F_{1,371}$ = 86.42, P < 0.001) but no interaction ($F_{6,371}$ = 1.08, P = 0.375) on adjusted grip force. After this adjustment, post hoc tests demonstrated that application of the nanomesh material has no effect on the grip force across all conditions compared with the bare finger (all comparisons P = 1.0). Even though the parylene film is thinner, the friction-adjusted grip force was increased compared with the bare finger (all comparisons P < 0.01), with a mean (±SEM) increase in friction-adjusted grip force of 13.8 ± 3.3%. Therefore, application of the nanomesh material was not found to interfere with the sensorimotor processing of object grasping, whereas materials of similar thickness (parylene) do affect this processing.

The nanomesh material can be used to measure grasping force with the sensors directly attached to the index finger. To avoid the effect of skin capacitance, we added a shielding layer and an Au nanomesh shield electrode layer (figs. S14 and S15). We compared the capacitance change in the nanomesh sensor with forces measured by a commercial (Nano 25, ATI) force sensor (fig. S16). While pressing on the force sensor with the nanomesh-attached finger, we simultaneously measured the capacitance change in nanomesh sensor

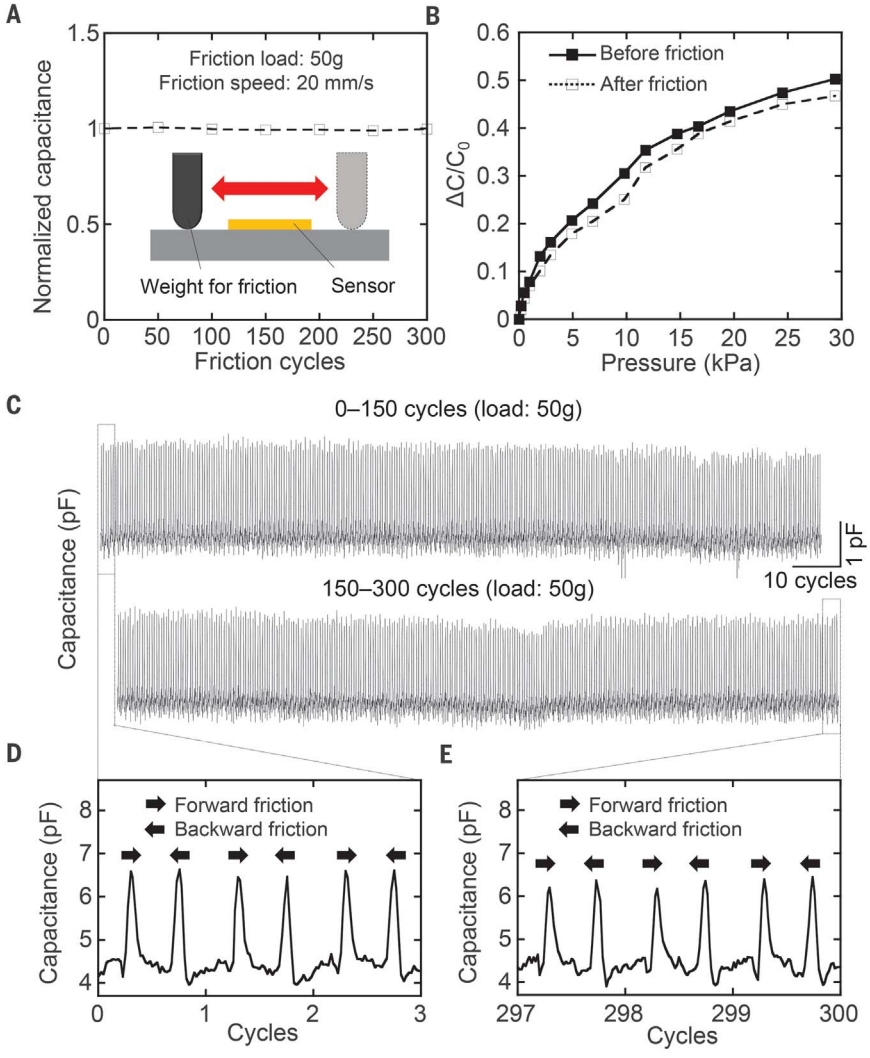

Fig. 3. Durability of the nanomesh sensor against friction. (**A**) Normalized capacitance of the device after the application of friction. The capacitance (initial capacitance without pressing) is normalized by the capacitance before application of friction. The sensor surface is rubbed by a spherical polyurethane ball with a weight of 50 g with a friction speed of 20 mm/s. The red arrow represents the direction of friction (forward and backward friction) for each cycle. (**B**) Pressure sensitivity before the friction test and after 300 cyclic frictions. (**C** to **E**) Dynamic capacitance change during cyclic friction applications.

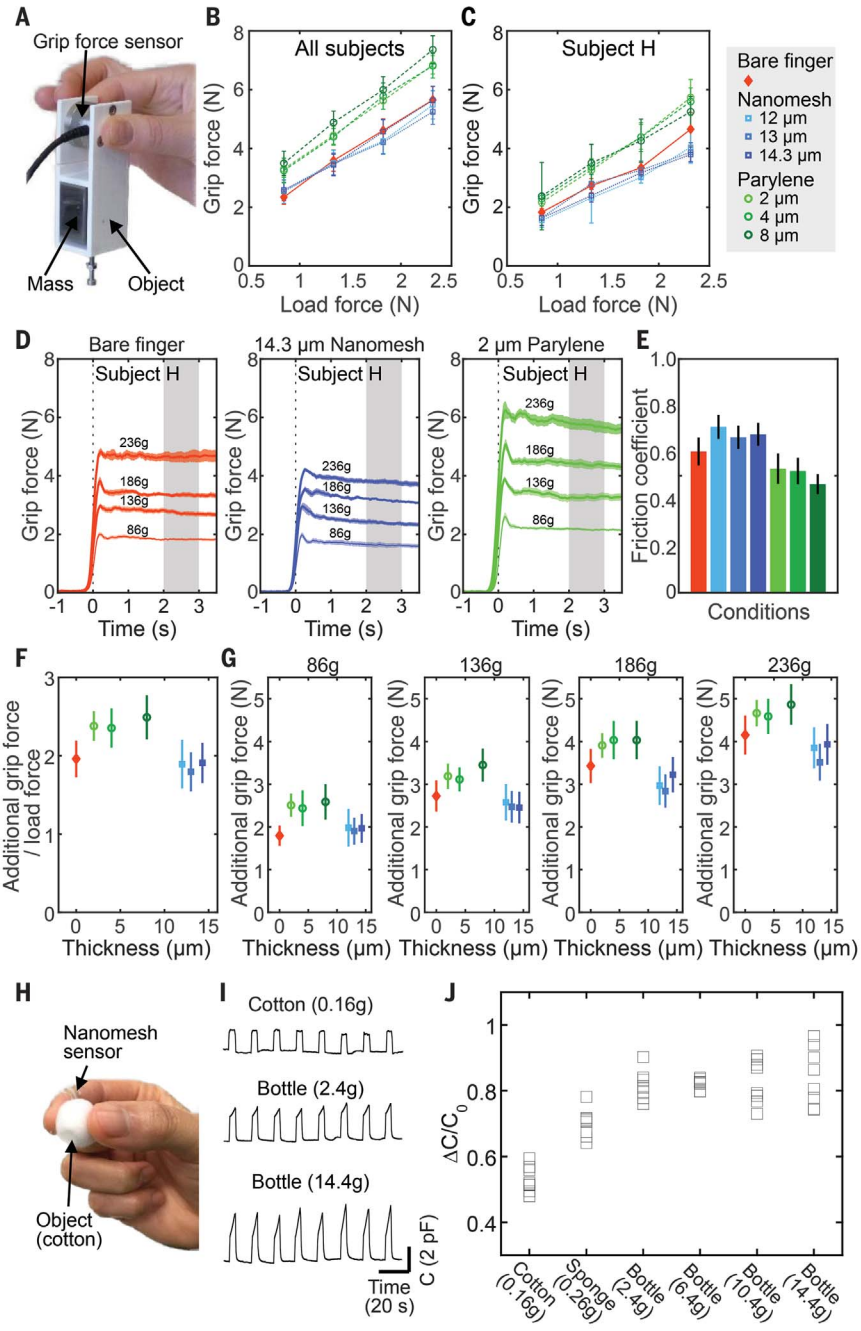

Fig. 4. The effects on human sensation caused by sensor attachment and force monitoring using the nanomesh sensor attached on finger. (**A**) Participants with seven different surface conditions on the index finger lift an object with four different masses that measures grip force. (**B**) Grip force (mean ± SEM) scaled with the load force across all participants. Nanomesh material on the index finger (blue) did not affect this relation compared with the bare finger (red). (**C**) Same relation shown for a single participant. (**D**) Grip force as a function of time (from object liftoff) for the different object masses for a single participant with bare finger, 14.3-μm nanomesh, and 2-μm parylene conditions. The shaded region indicates SEM. The gray-shaded area shows the time over which the grip force was measured for analysis. (**E**) Estimated friction coefficient between the finger and the object under the seven different surface conditions (color indicates condition). (**F**) Friction-adjusted additional grip force (exerted grip force minus minimum grip force, according to object friction) divided by load force plotted as a function of surface material thickness. Despite increased thickness, all nanomesh materials show similar adjusted grip force to the bare finger. (**G**) Additional grip force as a function of material thickness, as shown for each object mass separately. (**H**) A participant grasps a natural object (e.g., cotton ball) while the nanomesh sensor measures the grip force. (**I**) Capacitance as a function of time as the participant grasps different objects (cotton ball and small plastic bottles). (**J**) Nanomesh sensor measurement of grip force for six different natural objects. Each square indicates the peak value of one lift.

and the force change in the force sensor. The test consisted of repetitive cycles in which the force was applied for 5 s and released for 5 s, and the applied finger force gradually increased between repetitions. The nanomesh sensor exhibited the capacitance change in a similar fashion to the various finger forces, demonstrating the ability to measure finger force by using the nanomesh sensor. To show this capability in daily activities, we measured the precision grip while lifting an object. Objects, including a cotton ball, a cubic sponge, and bottles of different weights, were repeatedly lifted for 3 s and released for 12 s. Using the repeated capacitance changes for each object, we show an increase in the grip force, as measured by the nanomesh sensor, due to different shape or weights of objects (Fig. 4, H to J, and fig. S17), although there are trial-by-trial variations owing to feedforward planning (*33*) and motor noise (*34*).

We have demonstrated the monitoring of finger force without detectable effects on human sensation. The nanomesh sensors exhibit mechanical durability against shearing and friction while the ultrathin compliant structure preserves human sensitivity. Simultaneous achievement of imperceptible operation and superior durability opens the possibility of pressure monitoring in applications that require precise and continuous monitoring of motions in natural states. To improve the accuracy of estimated force, an increased number of pressure sensors and acquisition of a spatial pressure distribution will be needed. The development of stretchable and/or water-

resistive pressure sensors would further enhance the stability of sensors and enable a long-term pressure monitoring of finger and other biological objects. (figs. S18 and S19).

REFERENCES AND NOTES

1. A. Chortos, J. Liu, Z. Bao, *Nat. Mater.* **15**, 937–950 (2016).
2. H. Zhao, K. O'Brien, S. Li, R. F. Shepherd, *Sci. Robot.* **1**, eaai7529 (2016).
3. T. Yamada *et al*., *Nat. Nanotechnol.* **6**, 296–301 (2011).
4. C. Wang *et al*., *Nat. Mater.* **12**, 899–904 (2013).
5. G. J. Snoek, M. J. IJzerman, F. A. C. G. in 't Groen, T. S. Stoffers, G. Zilvold, *Spinal Cord* **38**, 244–249 (2000).
6. F. J. Valero-Cuevas, *J. Biomech.* **38**, 673–684 (2005).
7. N. Jowett, V. LeBlanc, G. Xeroulis, H. MacRae, A. Dubrowski, *Am. J. Surg.* **193**, 237–242 (2007).
8. A. Erol, G. Bebis, M. Nicolescu, R. D. Boyle, X. Twombly, *Comput. Vis. Image Underst.* **108**, 52–73 (2007).
9. S. A. Mascaro, H. H. Asada, *IEEE Trans. Robot. Autom.* **17**, 698–708 (2001).
10. Y. Sun, J. M. Hollerbach, S. A. Mascaro, *IEEE Trans. Biomed. Eng.* **55**, 2363–2371 (2008).
11. A. Naceri *et al*., *J. Neurophysiol.* **117**, 2025–2036 (2017).
12. M. Santello, M. Flanders, J. F. Soechting, *J. Neurosci.* **18**, 10105–10115 (1998).
13. L. Dipietro, A. M. Sabatini, P. Dario, *IEEE Trans. Syst. Man Cybern. C* **38**, 461–482 (2008).
14. J. Lee *et al*., *Adv. Mater.* **27**, 2433–2439 (2015).
15. S. Sundaram *et al*., *Nature* **569**, 698–702 (2019).
16. E. Battaglia *et al*., *IEEE Trans. Haptics* **9**, 121–133 (2016).
17. S. Gong *et al*., *Nat. Commun.* **5**, 3132 (2014).
18. A. P. Gerratt, H. O. Michaud, S. P. Lacour, *Adv. Funct. Mater.* **25**, 2287–2295 (2015).
19. Y. Gao *et al*., *Adv. Mater.* **29**, 1701985 (2017).
20. C. Dagdeviren *et al*., *Nat. Commun.* **5**, 4496 (2014).
21. Y. Cao *et al*., *Small* **14**, e1703902 (2018).
22. S. Lee *et al*., *Nat. Nanotechnol.* **11**, 472–478 (2016).
23. D. H. Kim *et al*., *Science* **333**, 838–843 (2011).
24. M. Kaltenbrunner *et al*., *Nature* **499**, 458–463 (2013).
25. Y. Tetsu *et al*., *Appl. Phys. Express* **10**, 087201 (2017).
26. M. Kondo *et al*., *Sci. Adv.* **6**, eaay6094 (2020).
27. G. Westling, R. S. Johansson, *Exp. Brain Res.* **53**, 277–284 (1984).
28. C. K. Bensel, *Ergonomics* **36**, 687–696 (1993).
29. A. Kopka, J. M. Crawford, I. J. Broome, *Acta Anaesthesiol. Scand.* **49**, 459–462 (2005).
30. S. Bilaloglu *et al*., *J. Neurophysiol.* **115**, 1122–1131 (2016).
31. A. Miyamoto *et al*., *Nat. Nanotechnol.* **12**, 907–913 (2017).
32. R. S. Johansson, J. R. Flanagan, *Nat. Rev. Neurosci.* **10**, 345–359 (2009).
33. R. J. van Beers, *Neuron* **63**, 406–417 (2009).
34. A. A. Faisal, L. P. J. Selen, D. M. Wolpert, *Nat. Rev. Neurosci.* **9**, 292–303 (2008).

ACKNOWLEDGMENTS

We thank T. Sakurai, Y. Ukiya, T. Mori, M. Sudama, S. Nagai, and M. Mori of the University of Tokyo (Japan) for the technical support and fruitful discussions. We also thank F. Bergner, K. Stadler, and S. Stenner of the Technical University of Munich (Germany) for technical support with the experimental device. **Funding:** This work was supported by the Japan Science and Technology (JST) ACCEL (grant number JPMJMI17F1), Japan Society for the Promotion of Science (JSPS) KAKENHI (grant number 17H06149), and the Technische Universität München – Institute for Advanced Study, funded by the German Excellence Initiative (and the European Union Seventh Framework Programme under grant agreement n° 291763). **Author contributions:** S.L., F.A.H., M.O.G.N., and Y.W. fabricated the nanomesh devices. S.L., F.A.H., M.O.G.N., Y.W., T.Y., and T.S. contributed the electric and mechanical characterizations and analysis of the nanomesh devices. S.F., R.L., G.C., and D.W.F. contributed to the evaluation of the effect on human sensation caused by sensor attachment. S.L., S.F., R.L., and D.W.F. performed the calibration and measurement of natural objects. S.L., S.F., F.A.H., D.W.F., and T.S. wrote the manuscript. T.S. supervised this project. **Competing interests:** The authors declare no competing interests. **Data and materials availability:** All data supporting the findings of this study are included within either the paper or the supplementary materials.

SUPPLEMENTARY MATERIALS

science.sciencemag.org/content/370/6519/966/suppl/DC1
Materials and Methods
Figs. S1 to S19
References (*35*–*40*)

24 May 2020; accepted 15 October 2020
10.1126/science.abc9735

Nanomesh pressure sensor for monitoring finger manipulation without sensory interference

Sunghoon Lee, Sae Franklin, Faezeh Arab Hassani, Tomoyuki Yokota, Md Osman Goni Nayeem, Yan Wang, Raz Leib, Gordon Cheng, David W. Franklin and Takao Someya

Science **370** (6519), 966-970.
DOI: 10.1126/science.abc9735

A soft touch

Measuring the force it takes for a hand to grasp an object requires sensors to be placed on the fingertips, but these sensors will interfere with or affect how much force ends up being applied. Lee *et al.* developed a nanomesh sensor built from a series of electrospun materials (see the Perspective by Liu). Using a robotic tester, they show that this device can repeatably detect the pressure involved in gripping an object. They also show that the sensors can be attached to human fingers and that this does not affect the force used to grasp an object.

Science, this issue p. 966; see also p. 910